Published in final edited form as:
Eur J Immunol. 2008 February ; 38(2): 550–564. doi:10.1002/eji.200737777.

SLIC-1/Sorting Nexin 20: A novel sorting nexin that directs subcellular distribution of PSGL-1

Ulrich Y Schaff[1,#], **Heather H Shih**[2,#], **Meike Lorenz**[4], **Dianne Sako**[3], **Ron Kriz**[4], **Kim Milarski**[2], **Brian Bates**[2], **Boris Tchernychev**[2], **Gray D. Shaw**[2], and **Scott I Simon**[1,*]

[1]Department of Biomedical Engineering, University of California Davis 451. E. Health Sciences Drive, Davis, CA 95616

[2]Biological Technologies Wyeth Research 87 CambridgePark Drive, Cambridge, MA 02140

[3]Department of Cardiovascular and Metabolic Diseases Wyeth Research 87 CambridgePark Drive, Cambridge, MA 02140

Abstract

PSGL-1 is a mucin-like glycoprotein expressed on the surface of leukocytes that serves as the major ligand for the selectin family of adhesion molecules and functions in leukocyte tethering and rolling on activated endothelium and platelets. Previous studies have implicated the highly conserved cytoplasmic domain of PSGL-1 in regulating outside-in signaling of integrin activation. However, molecules that physically and functionally interact with this domain are not completely defined. Using a yeast two-hybrid screen with the cytoplasmic domain of PSGL-1 as bait, a novel protein designated SLIC-1 (Selectin Ligand Interactor Cytoplasmic-1) was isolated. Computer-based homology search revealed that SLIC-1 was the human ortholog for the previously identified mouse sorting nexin 20. Direct interaction between SLIC-1 and PSGL-1 was specific as indicated by co-immunoprecipitation, and motif mapping. Co-localization experiments demonstrated that SLIC-1 contains a Phox homology (PX) domain that binds phosphoinositides and targets the PSGL-1/SLIC-1 complex to endosomes. Deficiency in the murine homologue of SLIC-1 did not modulate PSGL-1 dependent signaling nor alter neutrophil adhesion through PSGL-1. We conclude that SLIC-1 serves as a sorting molecule which cycles PSGL-1 into endosomes with no impact on leukocyte recruitment.

Keywords

Leukocytes; Selectins; Cell Surface Molecules; Protein Trafficking

Introduction

The initial tethering and rolling of leukocytes on activated endothelium and platelets is a key biological event mediated by PSGL-1, a mucin-like glycoprotein that functions as a unique high-affinity ligand for the selectin family of adhesion molecules (for reviews, see [1-4]). Structurally, PSGL-1 is a type I integral membrane protein consisting of a N-terminal selectin-binding domain followed by a region of multiple decameric repeats bearing O-linked glycans, a short transmembrane domain, and lastly a cytoplasmic tail [5-10]. Comparison of human and murine PSGL-1 reveals that the 69-amino acid intracellular

[*]Corresponding Author: Scott I. Simon Tel: 530-752-1430 #Fax: 530-754-5739 sisimon@ucdavis.edu.
[4]Current address: Non-Clinical Research and Development, ALZA Corporation 1900 Charleston Rd, Mountain View, CA 94039
[#]U. Schaff and H. Shih contributed equally to this work

domain of PSGL-1 is highly conserved. While overall identity between human and murine PSGL-1 is 50%, their cytoplasmic domains share 76% identity.

Several important physiological functions have been linked to the cytoplasmic domain of PSGL-1. First, it transduces signals from activated PSGL-1 into the cytoplasm of leukocytes, leading to downstream events including tyrosine phosphorylation of intracellular proteins [11], activation of integrin CD11b/CD18 [12], and induction of IL-8 [13]. Second, it modulates the adhesive properties of leukocytes. Truncation of the intracellular domain of PSGL-1 results in impaired rolling of myeloid cells on P-Selectin, presumably due to a loss of moesin- mediated association of PSGL-1 with the leukocyte cortical cytoskeleton [14]. Third, the cytoplasmic tail of PSGL-1 may contain determinants that target PSGL-1 to specific cell membrane domains. In resting leukocytes, PSGL-1 is restricted to the tips of microvilli, which facilitates its binding to selectins on other cells [15-17]. Despite the importance of these molecular and cellular functions mediated by the cytoplasmic domain of PSGL-1, the complete set of intracellular molecules that bind to the PSGL-1 cytoplasmic domain remain to be identified.

We report here on the isolation and initial characterization of a novel sorting nexin that specifically interacts with the cytoplasmic domain of PSGL-1, a protein we designate SLIC-1 for Selectin Ligand Interactor Cytoplasmic-1. The sorting nexins are a family of trafficking molecules defined by the presence of a Phox homology (PX) domain (for recent reviews, see[18-20]). Originally identified in the $p40_{phox}$ and the $p47_{phox}$ subunit of NADPH oxidase, the ~120-amino acid PX domain has been subsequently recognized in a number of proteins including sorting nexins and signaling molecules such as PI-3 kinase and CISK [21-33]. The PX domain has also been characterized as a phosphoinositide-binding module that can localize both the host protein and a bound protein to the cell membrane or intracellular vesicles (for reviews, see [20,34-36]).

A database homology search revealed that SLIC-1 was a member of the sorting nexin family. SLIC-1 contained a functional phosphoinositol-binding PX domain and could redistribute PSGL-1 to endosomes in cells. Functional significance of deletion of the SLIC-1 homologue in mice revealed that it did not affect neutrophil recruitment to the inflamed endothelium, indicating that the lack of SLIC-1 was not sufficient to modulate PSGL-1 function *in vivo*. This is the first report of the interaction of PSGL-1 with a sorting nexin, providing new insight into the intracellular trafficking of PSGL-1.

Results

Isolation of SLIC-1

To identify proteins that interact with the cytoplasmic domain of PSGL-1, a yeast two-hybrid screen was carried out using the cytoplasmic domain of human PSGL-1 as bait and cDNA library from human monocytic U-937 cells as prey. Two specific molecules were isolated, both of which were novel proteins. This study characterized one of these two proteins, which we named SLIC-1 for Selectin Ligand Intracellular Cytoplasmic −1. A partial cDNA sequence derived from the yeast two-hybrid screen was used to screen a lambda ZAPII U937 cell cDNA library to identify a full-length coding sequence for SLIC-1 (Fig. 1A, GenBank accession no. AY302441). Northern blot analysis using SLIC-1 cDNA probe revealed a 3-Kb mRNA species present in various tissues of hematopoitic origin as well as liver, small intestine, placenta, and lung (Fig S1).

The open reading frame in *SLIC-1* cDNA encoded a protein of 316 amino acids with a predicted molecular weight of 36 kDa (Fig. 1A). Amino acid analysis of SLIC-1 revealed a centrally located domain that was homologous to the Phox homology (PX) domain (shaded

amino acids in Fig. 1A. In addition to the PX domain, SLIC-1 had a proline-rich N-terminus containing three PXXP motifs (amino acids in bold in Fig. 1A), which are potential SH3 domain-interacting motifs. The region C-terminal to PX domain consisted of 128 amino acids and did not show homologies to any known motifs. Nucleotide sequence analyses by BLAST search revealed sequence homology to a murine protein called SNX20 and a human protein called SNX21/SNX-L (Fig. 1B). SNX20 and SNX21/SNX-L were proteins identified in efforts to isolate new sorting nexins based on the homology of their PX domains [20,37]. When aligned by BLAST program, SLIC-1 and SNX20 shared 77% identity and 84% homology, while SNX20 and SNX21/SNX-L shared 38% identity and 52% homology. The alignment results suggested that SNX20 is the mouse homologue of SLIC-1. Based on mouse genomic sequence of SLIC-1 (unpublished data), we cloned mouse SLIC-1 cDNA by RT-PCR using mRNA extracted from mouse monocytic WEHI cells and confirmed that the mouse homologue of SLIC1 was indeed SNX20 (data not shown). Despite the structural similarities to sorting nexins, the functions for SNX20 or SNX21/SNX-L have not been defined.

Interaction of SLIC-1 with PSGL-1 in mammalian cells

To confirm that interaction of PSGL-1 and SLIC-1 as observed in yeast occurs in mammalian cells, these molecules were co-immunoprecipitated from COS cells co-transfected with plasmids encoding SLIC-1 and PSGL-1. Immunoprecipitation of transfected lysates was performed using a mouse monoclonal anti-human PSGL-1 antibody and a control mouse IgG. SLIC-1 was detected in the PSGL-1 immunocomplex but not in the control immunocomplex by Western analysis (bands indicated by arrows in Lanes 1-2, top SLIC-1 blot, Fig. 2B). These data demonstrated that PSGL-1 and SLIC-1 interact specifically in mammalian cells.

To confirm that the interaction was specific for the cytoplasmic domain of PSGL-1, plasmids encoding mutant PSGL-1 were constructed (Fig. 2A). Two mutants were expressed: pMT-PSGLΔCT lacked the cytoplasmic domain, whereas a control mutant pMTPSGL/L-SECT contained L-Selectin cytoplasmic domain in place of PSGL-1 cytoplasmic domain. The rationale for making the latter mutant was to test whether SLIC-1 specifically interacted with PSGL-1 among cell surface molecules that assume similar membrane localization. In resting leukocytes, both PSGL-1 and L-Selectin localize to the tips of microvilli [15-17,38-40]. Despite being expressed at similar levels as the wildtype PSGL-1 (Lanes 3-4, PSGL-1 blots in Fig 2B), both PSGLΔCT and PSGL/L-SECT showed little association with SLIC-1 (Lanes 3-4, top SLIC-1 blot in Fig. 2B), demonstrating that the interaction of PSGL-1 with SLIC-1 was specifically mediated by the cytoplasmic domain of PSGL-1.

To map the SLIC-1 binding domain, a truncation mutant of PSGL-1 was made and tested in the co-immunoprecipitation assay. Deletion of the most C-terminal 42 amino acids (PSGL360, Fig. 3A) yielded binding activity comparable to or slightly higher than wildtype PSGL-1 (Compare Lane 5 to Lane 1 and Lane 8 to Lane 6, top SLIC-1 blot in Fig. 2B), suggesting that SLIC-1 binding domain is within the first 37 amino acids in the PSGL-1 cytoplasmic domain. It has been reported that the ERM proteins moesin and ezrin directly bind the cytoplasmic domain of PSGL-1 [41,42]. The binding site has been mapped to a juxtamembrane region within PSGL360 comprising the amino acid sequence of SRKGH and S348 (61) (underlined amino acid sequence in Fig 2A).[42] To investigate the relationship between ERM binding and SLIC-1 binding, mutant PSGL-1 on the background of PSGL360 was generated with ERM binding sequence mutated (PSGL360Δ including SRKGH deletion and S348A mutation, Fig. 2A). Interestingly, this mutant exhibited enhanced SLIC-1 binding activity compared to either wildtype PSGL-1 or PSGL360 (compare Lane 9 to Lane 6 and Lane 8, top SLIC-1 blot in Fig. 2B), suggesting that the

endogenous ERM proteins in COS cells might compete for SLIC-1 binding to the cytoplasmic domain of PSGL-1. We next sought to confirm the above results in an *in vitro* motif mapping experiments by peptide array analysis. Arrays of 12-amino acid peptides were directly synthesized onto cellulose membranes. The entire peptide array constituted overlapping amino acid sequences (i.e. differing by only one amino acid), spanning PSGL-1 cytoplasmic domain. The array was probed with bacterially expressed and purified GST-SLIC-1 fusion protein for positive interactions. As shown in the top panel in Fig. 2C, peptides that showed positive interaction with GST-SLIC-1 comprised sequences from two regions of PSGL-1 cytoplasmic domain: a transmembrane (TM) proximal motif (YPVRNYSPTEM) and a TM distal motif (SPGLTPEPREDREGDDLTLHSFLP). Interestingly, in the co-immunoprecipitation assay, PSGL360 bound SLIC-1 as avidly as wildtype even though it spanned only the TM proximal motif. We also probed the peptide array with the PX domain of SLIC-1 fused C-terminally to GST (GST-PXSLIC). This protein displayed the same binding profile as GST-SLIC-1, interacting with both the TM proximal motif (YPVRNYSPTEMV) and the TM distal motif (SPGLTPEPREDREGDDLTLHSF) in PSGL-1 cytoplasmic domain (middle panel, GST control did not show any binding to the peptide array (bottom panel, Fig. 2C), demonstrating the specificity of the assay. To confirm the results from peptide array analysis, a BIACORE was used to assay SLIC-1 recognition of two synthesized peptides that showed positive binding to GST-SLIC-1 (HMYPVRNYSPTE, REDREGDDLTLH). Both peptides showed specific and saturable binding to GST-SLIC-1 (Fig S2). Taken together, these *in vitro* studies revealed that SLIC-1 bound PSGL-1 via its PX domain and two binding motifs in the cytoplasmic domain.

(Section relating to Fig 2D deleted)

Localization of SLIC-1 to endosomes in COS cells

A number of PX domain-containing proteins including sorting nexins have been found to localize to the endosomal compartments of cells (e.g. [24,33]). Heterologous systems including COS cells have been employed to examine the subcellular localization of these proteins [21,30]. When EGFP-SLIC-1 was expressed in COS cells, similar subcellular distribution was observed as in K562 cells. SLIC-1 was found to localize to cell membrane, cytosol, nucleus, and intracellular vesicles (green staining in Fig. 3A & 3D). The basis for the nuclear localization was not clear, since computer analysis did not predict any recognizable nuclear import sequence. The vesicular structures where SLIC-1 resided were reminiscent of the endosomal compartments of other PX domain-containing molecules including several sorting nexins reside (e.g. [21,30]). Two endosomal markers, early endosomal antigen-1 (EEA-1) and endocytosed transferring, were used in co-localization experiments to confirm the endocytic nature of these vesicles. In both cases, SLIC-1 co-localized with EEA-1 (Fig. 3C) or transferrin in endosomes (Fig. 3F). These results demonstrated that SLIC-1 localized to endosomes in cells.

The PX domain of SLIC-1 is a functional lipid-binding domain

The PX domain is capable of targeting its host protein to endosomes by binding to PtdIns(3)P, a phosphoinositol important to endosomal structure and function in resting cells. Alignment of SLIC-1 PX domain with other PX domains revealed high degree of preservation of conserved amino acids (Fig. 4A), suggesting that SLIC-1 PX domain would be a functional lipid-binding module. Bacterially expressed and purified GST-SLIC$_{PX}$ was used to examine its lipid-binding activities in an overlay assay. Positive interaction of SLIC-1 PX domain with a subset of phospholipids was detected, which included PtdIns(3)P, PtdIns(4)P, PtdIns(5)P, PtdIns(3,4)P_2, and PtdIns(3,5)P_2, and PtdIns(3,4,5)P_3 (left panel, Fig. 4B). The binding was specific for SLIC-1 PX domain since GST alone did not produce

any binding activity (data not shown). Similar results were obtained in a lipid overlay assay using a commercial lipid array with serial dilutions of lipids spotted onto nitrocellulaose membrane (Left panel, Fig. 4C). Weak interactions with PtdIns(3)P and PtdIns(3,4,5)P_3 were detected after long exposure on the lipid array (data not shown).

The crystal structure of p40phox bound to PtdIns(3)P has recently been solved and Arg58 in p40phox was shown to form the most extensive interaction with the bound phospholipid [43]. A single amino acid mutation to Gln at this position was reported to effect loss of phospholipid binding without affecting the overall fold of the protein. This residue was highly conserved throughout PX domain containing proteins and was present as Arg116 in SLIC-1. This prompted us to produce a mutant GST-PXSLIC protein containing an analogous Arg-to-Gln mutation at this position (R116Q). This resulted in decreased binding activity to all phospholipids as compared to wildtype $GSTPX_{SLIC}$ (compare the right panel with the left panel in Fig. 4B and Fig. 4C, respectively), while the two proteins were expressed at similar levels (Fig. 4D). This result suggested that the PX domain of SLIC-1 used conserved mechanisms to bind phospholipids.

Phospholipid binding is required for SLIC-1 localization to endosomes

Since the R116Q mutation decreased binding of SLIC-1 PX domain to phospholipids *in vitro*, we asked whether this mutation in full-length SLIC-1 would alter subcellular targeting of SLIC-1 to endosomes in cells. A plasmid encoding EGFP-SLICR116Q was constructed and expressed in COS cells. Impressively, none of the COS cells expressing the mutant showed localization of this protein to endocytic vesicles, while plasma membrane and nuclear localization of SLIC-1 was not affected (bottom panel, Fig. 5A). Compared to decreasing lipid binding *in vitro* (Fig. 4B and C), the R116Q mutation manifested a more potent phenotype in cells, presumably due to the presence of limited amount of phospholipids in endosomal membranes in cells. This SLIC-1 mutant was capable of specifically interacting with PSGL-1 in a co-immunoprecipitation assay (data not shown), indicating that this mutation did not disrupt the overall protein folding. We next examined whether the endosomal targeting of SLIC-1 was mediated through the binding of its PX domain to endogenous phospholipids in the endosomes. Since the production of PtdIns(3)P in endosomes in COS cells is controlled by PI-3 kinase, the effect of inhibiting PI-3 kinase activity on SLIC-1 subcellular distribution was subsequently examined. COS cells transfected with EGFP-SLIC-1 expressing plasmid were treated with the PI-3 kinase inhibitor Wortmannin for indicated periods of time before they were fixed for analysis by fluorescent microscopy. As shown in Fig. 5B, in untreated cells, endosomal localization of SLIC-1 was observed in every EGFP-SLIC-1 expressing cell (arrowheads in 0 min panel, Fig. 5B). After 30 min of Wortmannin treatment, SLIC-1 was no longer localized to the endosomes (disappearance of vesicles in 30-min and 40-min panels, Fig. 5B), while the prominent nuclear distribution was preserved in the EGFP-SLIC-1-expressing cells. Taken together, these results suggested that the PX domain targeted the endosomal localization of SLIC-1 by binding to endogenous PtdIns(3)P on endosomal membranes in COS cells.

Co-expression of SLIC-1 with PSGL-1 regulates subcellular distribution of PSGL-1

Since the mouse homologue of SLIC-1, SNX20, was classified as a *bona fide* sorting nexin, we tested whether SLIC-1 functioned as a sorting nexin to modulate the trafficking of PSGL-1. We expressed EGFP-SLIC-1 in CHO cells that constitutively expressed human PSGL-1 [44] and examined the subcellular localization of PSGL-1 by confocal microscopy following indirect immunofluorescent staining. Similar to untransfected cells or cells expressing EGFP protein (data not shown), PSGL-1 localized to plasma membrane as well as cytoplasm in cells transfected with EGFP-SLICRQ (Fig. 6A. d). Expression of EGFP-SLIC-1 caused a striking re-distribution of PSGL-1 to SLIC-1-residing endosomes (Fig. 6A.

a, c). When counted under fluorescent microscope, 70% of EGFP-SLIC-1 expressing cells showed endosomal PSGL-1 staining (Fig. 6B, left bar), while 10% of EGFP-SLIC116Q expressing cells exhibited PSGL-1 staining in vesicles (Fig. 6B, right bar). Importantly, only one or two PSGL-1 positive vesicles were observed in EGFP-SLIC116Q-expressing cells, while a large number of vesicles were found in EGFP-SLIC-1-expressing cells (Fig. 6A. a). The targeting of PSGL-1 to the endosomes was dependent on a functional PX domain in SLIC-1, since co-expression of SLICR116Q mutant with PSGL-1 abrogated its detection in the endosomes (Fig. 6A. d and 6B). This was observed despite the fact that these two proteins were still capable of physical interaction in co-immunoprecipitation experiments (data not shown). Furthermore, expression of EGFP-SLIC-1 in a CHO cell line constitutively expressing a soluble form of PSGL-1 truncated after Ile316 (sPSGL) inhibited re-distribution of sPSGL to the endosomes (data not shown). These results indicated that the interaction of SLIC-1 with the cytoplasmic domain of PSGL-1 resulted in altered subcellular localization of PSGL-1. Sorting nexins such as SNX1 are known to target cell surface proteins for lysosomal degradation. Although SLIC-1 caused extensive re-distribution of PSGL-1 to endosomes, membrane expression of PSGL-1 remained unchanged when SLIC-1 was co-expressed indicating that SLIC-1 did not enhance the degredation of PSGL-1 (Fig S3). Moreover, the absence of the murine homologue of SLIC-1 in SNX20 knockout mice (see below) did not alter membrane expression of PSGL-1 in leukocytes from bone marrow cells as determined by FACS analysis (Fig S3).

Deletion of murine homologue of SLIC-1, SNX20, does not affect PSGL-1-dependent signaling in murine neutrophils

In response to local inflammation, the endothelial walls of venules upregulate E-selectin which binds PSGL-1 among other sialylated ligands on leukocytes. This subsequently leads to the activation of integrins on the activated leukocytes. Because PSGL-1 is known to act as an adhesive signaling molecule in murine neutrophils, we tested whether the interaction between SLIC-1 and PSGL-1 might serve a signaling role during neutrophil recruitment to the inflamed endothelium. Specifically we investigated whether neutrophil adhesion as a result of β2-integrin activation triggered via E-selectin ligation and membrane clustering of PSGL-1 was dependent on the presence of SLIC-1.

Mice deficient in SNX20, the murine homologue for human SLIC-1, were generated in the 129SvEvBrd background. Exons 2 and 3 of SNX20 gene including the transcription initiation codon ATG were deleted (Supplemental material). These mice were overall normal and healthy. Our first attempt to determine a functional output of SLIC-1 was to employ mouse neutrophils deficient in SNX20 in a vascular mimetic flow chamber. To observe integrin activation stemming directly from E-selectin ligation under shear stress as previously reported [45], we replicated the geometry of a post-capillary venule in a custom-made flow chamber. Neutrophils were isolated from murine bone marrow and perfused over an L-cell monolayer expressing E-selectin and ICAM-1 (L-E/I). As shown in Fig. 7, over time, an increasing portion of the wildtype neutrophils exhibited integrin activation as indicated by an increase in the fraction of adherent and arrested neutrophils. As compared to the wildtype neutrophils, SNX20−/− neutrophils exhibited similar behavior under these experimental settings. Both the density of neutrophils recruited per unit area and the fraction of these captured neutrophils that converted to arrest remained similar between SNX20-deficient and wildtype neutrophils (Fig. 7). These results indicate that the absence of SNX20 is not sufficient to affect PSGL-1-dependent capture and signaling of neutrophil arrest on E-selectin and ICAM-1.

A hallmark of selectin dependent arrest is the redistribution of surface PSGL-1 into large, high density clusters [46]. Despite the lack of a clear role in selectin dependent neutrophil activation and arrest, it is possible that SNX20 has a role in this surface redistribution. To

investigate this possibility, we briefly labeled nonpermeabilized live murine neutrophils with antibody against PSGL-1, and imaged its distribution during neutrophil recruitment to the L-E/I monolayers. As shown in Fig. 8, in both wildtype and SNX20−/− neutrophils PSGL-1 rapidly formed characteristic clusters during rolling interaction with L-E/I. Detailed analysis of the size and distribution of these high density clusters revealed no difference in PSGL-1 topography. Subsequent to neutrophil arrest, PSGL-1 is known to redistribute to the trailing uropod of neutrophils migrating and transmigrating on inflamed endothelial cells [41]. No difference in PSGL-1 redistribution to the uropod was observed between WT and SNX20−/− neutrophils transmigrating through murine bEND.3 endothelial monolayer stimulated with IL-1β (Fig S4) [47]. Therefore the absence of SNX20 did not disrupt surface redistribution of PSGL-1 on rolling, activated, or transmigrating neutrophils.

The use of primary and secondary antibodies to crosslink PSGL-1 on a neutrophil surface is known to mimic direct ligation of PSGL-1 by selectins and can induce downstream events including calcium flux, F-actin polymerization, and integrin activation and affinity maturation [48,49]. To examine the potential participation of SNX20 in PSGL-1 dependent signaling, PSGL-1 was crosslinked on murine neutrophils loaded with the calcium sensitive dye Fluo-4. Influx of calcium served as a sensitive indicator of neutrophil activation state, and would reveal any defects in PSGL-1 dependent activation in SNX20 deficient neutrophils. Compared to the antibody, calcium flux was upregulated to a comparable level in both wildtype and SNX20−/− neutrophils upon PSGL-1 crosslinking (Fig. 9). Taken together our functional assays using murine SNX20−/− neutrophils reveal no defect in PSGL-1 dependent inflammatory signaling in neutrophils.

Discussion

The cytoplasmic domain of PSGL-1 is a highly conserved region that regulates the adhesion receptor's subcellular localization and immune functions. To date, the only proteins shown to directly interact with this region of PSGL-1 are the actin-binding proteins moesin and ezrin [41]. Here we report the isolation and identification of a novel protein called SLIC-1 that directly binds to the cytoplasmic tail of PSGL-1. Several lines of evidence collectively confirm the interaction between SLIC-1 and PSGL-1. First, SLIC-1 was isolated from the yeast two-hybrid screen via direct interaction with the cytoplasmic domain of PSGL-1. Second, a complex of PSGL-1 and SLIC-1 can be co-immunoprecipitated from cells over-expressing these proteins. Third, purified GST-SLIC-1 binds to peptides corresponding to sequences derived from PSGL-1 cytoplasmic domain in the peptide array analysis. Fourth, PSGL-1 and SLIC-1 co-localize in CHO cells expressing these two proteins. We have attempted to characterize the *in vivo* functional interactions between these two proteins by deleting the muringe homologue of SLIC-1, SNX20, from the mouse genome. However, the loss of SNX20 did not diminish the ability of PSGL-1 to mediate leukocyte tethering or rolling, nor activation of cell arrest via β_2-integrins.

SLIC-1 belongs to the family of sorting nexins that all contain a phospholipid-binding domain called the PX domain. The mammalian sorting nexin family currently includes 31 members [50]. In general, sorting nexins are believed to play a role in subcellular membrane and protein trafficking [50,51]. Several sorting nexins including SNX1 and SNX2 have been defined as components of a mammalian retromer complex functioning in the retrieval of cargos from the endosomal system to the Golgi. However, the function of the majority of this protein family remains unclear. SLIC-1/SNX20 belongs to a 13-member subgroup of sorting nexins that contain extra motifs outside the PX domain but with unclear functions [50] This study demonstrates that SLIC-1 localizes to early endosomes dependent on the phospholipids binding activity of its PX domain. Interaction of SLIC-1 with PSGL-1 leads to re-distribution of PSGL-1 to endosomes. As an integral membrane receptor, the

biogenesis of PSGL-1 involves post-translational modification in Golgi and post-Golgi sorting through endosomes to proper membrane location [52]. SLIC-1 may play a role in the post-Golgi trafficking of PSGL-1 by targeting PSGL-1 into sorting endosomes. Once SLIC-1 directs PSGL-1 to the proper location in the plasma membrane, it may subsequently "hand off" PSGL-1 to the ERM proteins for the anchorage of PSGL-1 in restricted cell membrane domains. The ERM proteins have been shown to actively modulate the cell membrane localization of PSGL-1 by directing its movement to the uropod in activated leukocytes through direct interaction with PSGL-1 cytoplasmic domain [59]. Intriguingly, SLIC-1 and ERM seem to compete for PSGL-1 binding since we have found that the SLIC-1 binding motifs in PSGL-1 are distinct from that of the ERM proteins, and mutating the ERM binding motif on PSGL-1 actually resulted in increased SLIC-1 binding. It is worth further dissecting the mechanisms of PSGL-1 regulation by SLIC-1 and ERM in future work.

One function linked to several sorting nexins is the regulation of recycling and degradation of cell surface receptors. For example, SNX17 has been reported to promote the membrane recycling of LRP by preventing the sorting of this receptor to lysosomes for degradation [53]. Our data does not support a role of SLIC-1 in the regulation of PSGL-1 recycling and/or degradation. Co-expression of SLIC-1 with PSGL-1 does not alter the steady-state levels of PSGL-1 and the deletion of mouse SLIC-1/SNX20 does not change PSGL-1 surface levels on leukocytes.

As PSGL-1 interacting proteins, the ERM proteins have been shown to function as adaptors to mediate PSGL-1 signaling by recruiting tyrosine kinase Syk to activated PSGL-1 [54]. We examined a possible role for SLIC-1 to mediate downstream signaling events from PSGL-1 by using mice containing the deletion of the gene encoding murine SLIC-1 homologue SNX20. Our results suggest that SLIC-1 may not play a signaling role downstream from PSGL-1 during neutrophil recruitment to inflamed endothelium. SNX20 deficient neutrophils rolling on a selectin-expressing substrate or stimulated with direct crosslinking of PSGL-1 showed no defect in activation and adhesive function. It is possible that the function of SLIC-1 is restricted to the regulation of the intracellular trafficking of PSGL-1, while the ERM proteins take over PSGL-1 from SLIC-1 at the plasma membrane and regulate the signaling functions of PSGL-1. Alternatively, a defect in PSGL-1-mediated signaling caused by the lack of SNX20 may be masked by the presence of additional selectin ligands that allow normal selectin interaction following initial leukocyte tethering. A third possibility is that a homologous protein to SNX20 called SNX21/SNX-L may substitute the function of SNX20 in the SNX20 deficient mice. Despite a vast number of reports on sorting nexins in recent years, gene deletion in mice have not been applied extensively to studying sorting nexins and up to date only three sorting nexins (*i.e.* SNX1, SNX2, and SNX13) have been deleted from mouse genome [55,56]. Interestingly, the deletion of SNX1 or SNX2 alone did not lead to any phenotype, but deletion of both revealed their functions in cellular trafficking[55]. This demonstrates that homologous sorting nexins can have redundant roles *in vivo* and deletion of a single sorting nexin may not readily yield functional phenotypes. This report is reminiscent of our study where the deletion of SNX20 alone has failed to manifest any regulation of PSGL-1 functions. The function of SNX20 homologue SNX21/SNX-L is largely unknown and so far we have not analyzed a possible interaction between SNX21 and PSGL-1. If they do interact, future attempts should be made to examine PSGL-1 signaling in SNX20/SNX21 doubly deficient mice.

In summary, we have identified a novel protein designated SLIC-1 that directly interacts with the cytoplasmic domain of PSGL-1 and targets PSGL-1 to endosomes in cells. The physiological functions of SLIC-1 could involve transport of newly synthesized PSGL-1 among intracellular compartments and/or specialized membrane domains. Future studies

will attempt to isolate an antibody that recognizes endogenous SLIC-1, thereby providing a tool to directly track its redistribution during modulation of leukocyte and endothelial function *in vivo*. Deletion of the murine homologue of SLIC-1 failed to alter PSGL-1 signaling, suggesting that either SLIC-1 does not play a role in PSGL-1 signaling, or other SLIC-1 homologues such as SNX21/SNX-L can play a redundant role in PSGL-1 sorting and signaling.

Methods and Materials

Yeast Two-hybrid Screen

To construct the bait vector, DNA fragment encoding the cytoplasmic domain of human PSGL-1 (PSLcyt) was amplified by PCR with the forward primer 5′-ATA CTG AAT TCC GCC TCT CCC GCA AGG GCC ACA T-3′ and the reverse primer 5′-ATA CAG GAT CCA GAG TGA GCT AAG GGA GGA AAG-3′ and cloned into pEG202 using EcoRI and BamHI restriction sites. This resulted in an in-frame insertion of DNA encoding PSGL-1 cytoplasmic domain fused 3′ to cDNA encoding the DNA binding protein LexA. The bait vector was transformed into the *S. Cerevisiae* yeast reporter strain EGY48 carrying the pSH18-34 lacZ reporter plasmid. Yeast carrying the PSLcyt bait protein was subsequently transformed with amplified DNA of a U937 cDNA library in the vector pJG4-5 and selected on CM/Ura-/His-/Tryp-/Leu-/X-Gal+ plates in the presence of galactose a and raffinose which allowed galactose-dependent gene transcription of proteins encoded by the cDNA library. Leu+/LacZ+ yeast clones were further tested to confirm the specificity of the two-hybrid interactions. Plasmids from clones that showed specific interactions were rescued and subjected to sequencing.

Full-length cDNA Cloning

Sequence analysis of yeast two-hybrid clones was done at DNA Sequencing Department at Wyeth. A partial cDNA sequence of SLIC-1 derived from the yeast two-hybrid screen was used to screen a lambda ZAPII U937 cell cDNA library to obtain the full length clone.

DNA Constructs

A 1.5-kB SalI DNA fragment containing the entire SLIC-1 coding region was subcloned into the SalI site of pEDΔC mammalian expression vector. A 950-bp fragment containing SLIC-1 coding region was generated by PCR with the forward primer 5′- CGG GAT CCG GAT CCA TGG CAA GTC CAG AGC ACC-3′ and reverse primer 5′-CGG GAT CCT CAG TGC AGG TAT TCT CGC-3′ and subcloned into the BamHI site of pEGFP-C1 (Clontech). PEGFP-SLICR116Q mutant was generated by over-lapping PCR mutagenesis. The first round of PCR was carried out using primer pair I (Primer A 5′- CGG GAT CCG GAT CCA TGG CAA GTC CAG AGC ACC-3′; Primer B 5′-GCG AAG TCG GAA TAT TGC CGT TCC AGG AC-3′) and primer pair II (Primer C 5′-GTC CTG GAA CGG CAA TAT TCC GAC TTC GC-3′; Primer D 5′-CGG GAT CCT CAG TGC AGG TAT TCT CGC-3′). The two products from the first round of PCR were purified from an agarose gel and combined in a second round of PCR using primer pair III (Primer A and Primer D) to obtain full-length SLIC-1 coding cDNA. The resulting DNA fragment was subcloned into BamHI site of pEGFP-C1. To generate pGEX-3X construct encoding the PX domain of SLIC-1, a 450-bp fragment encoding the PX domain of SLIC-1 was generated by PCR with the forward primer 5′-CGG GAT CCT TCA GTA CTG GCA GAA CCA G-3′ and the reverse primer 5′-CGG GAT CCT CAC ACG CGC AGC AGC AGC-3′ and subcloned into the BamHI site of pGEX-3X (Clonetech). To generate pGEX-3X construct encoding PXR116Q mutant PX domain of SLIC-1, mutant DNA was generated by PCR using pEGFP-C1-SLICR116Q plasmid as template. Same primers used to generate wildtype PX domain were used. The resulting PCR fragment was subcloned into the BamHI site of

pGEX-3X. PSGL-1 mutant constructs were generated by PCR and cloned in the EcoRI site of pMT21 mammalian expression vector. To generate pMT-PSGL/L-SECT, pMT-PSGL-1 was used as template in two consecutive PCR reactions using primers with sequences corresponding to DNA sequences encoding the cytoplasmic domain of L-Selectin. A first round of PCR reaction was carried out using the forward primer 5′-ATC CAC TTT GCC TTT CTC TCC-3′ (HS62) and the reverse primer 5′- ATA CTT CTC TTG GAT TTC TTG CCT TTT TTT AAT CTC CTG ACC GCC AGC ACC ACA GTG C -3′. The PCR product was gel purified and used as the template for a second round of PCR reaction using HS62 as the forward primer and the reverse primer 5′-CGG AAT TCG AAT TCT TAA TAT GGG TCA TTC ATA CTT CTC TTG GAT TTC TTG C-3′. The PCR product was subsequently cloned into the EcoRI site of pMT21. During this cloning, a mutant clone was generated that encoded a stop codon following two Arg residues immediately after the PSGL-1 transmembrane domain, which we named PSGLΔCT mutant. To generate pMT21-PSGL360 mutant, PCR reaction was carried out using HS62 as the forward primer and the reverse primer 5′- CGG AAT TCG AAT TCT AAG GCA ACA GGG ATG AGA TGC-3′. To generate PSGL360Δ mutant, PCR reaction was carried out using HS62 as the forward primer and the reverse primer 5′-CGG AAT TCG AAT TCT AAG GCA ACA GGG ATG AGA TGC AGA CCA TCT CGG TGG GGG C-3′. The sequences of all cloned constructs were verified by DNA sequencing.

Cell Culture and Transient Transfections

COS M6 cells were maintained in Dulbecco's modified Eagle's medium containing 10% heat-inactivated fetal bovine serum (Sigma), 2mM glutamine, 200 units/ml penicillin and 200units/ml streptomycin. A CHO cell line stably expressing PSGL-1 were previously established [44] and maintained in MEM⟨ medium containing 10% heat-inactivated and dialyzed fetal bovine serum, 1mg/ml G418 (Invitrogen), 10mM methotrexate (Sigma), 2mM glutamine, 200 units/ml penicillin and 200units/ml streptomycin. K562 cells were obtained from ATCC and were maintained in Iscove's modified Dulbecco's medium containing 10% heat-inactivated FCS, 4mM L-glutamine, 1.5g/L sodium bicarbonate, 200 units/ml penicillin and 200units/ml streptomycin. WEHI cells were obtained from ATCC and were maintained in Dulbecco's modified Eagle's medium containing 10% FCS, 4mM L-glutamine, 1.5g/L sodium bicarbonate, 200 units/ml penicillin and 200units/ml streptomycin. Transient transfection of COS M6 cells was carried out using LipofectAMINE2000 (Invitrogen) according to manufacturer's directions. Transient transfection of K562 cells was carried out using Tfx-50 reagent (Promega) according to manufacturer's directions.

Co-immunoprecipitation of SLIC-1 and PSGL-1

COS cells transiently transfected with expression vectors encoding SLIC-1 and wildtype or mutant PSGL-1 were lysed in lysis buffer [50 mM Tris-HCl, pH7.5, 150 mM NaCl, 1% Triton-X, 5mM EDTA, 5mM DTT with dissolved protease inhibitor tablet (Roche)]. Cell lysates were cleared by centrifugation and supernatants were collected. PSGL-1 immunoprecipitation was carried out using a mouse monoclonal antihuman PSGL-1 antibody 2G3 and protein G-agarose beads (Amersham). Control immunoprecipitation was carried out using mouse IgG (Santa Cruz). Immunocomplexes collected on the protein G-agarose beads were separated on 10% SDS-PAGE gel and subsequently transferred to PVDF membrane (Bio-Rad). Standard Western blotting procedures were carried out. To detect SLIC-1, a rabbit anti-SLIC-1 antibody raised against purified GST-SLIC-1 protein was used. On Western blots, this antibody recognized over-expressed SLIC-1 in cell lysates but not endogenous SLIC-1 To detect PSGL-1, a mouse monoclonal anti-human PSGL-1 antibody 4H10 was used.[57] Protein detection was achieved using an ECL Western blotting kit (NEN).

Expression and Purification of GST Fusion Proteins

E. Coli BL21 cells (Stratagene) were transformed with pGEX-3X encoding GST or pGEX-3X plasmids encoding full-length SLIC-1 and wildtype or mutant SLIC-1 PX domain, respectively. After reaching cell density of $O.D._{600}$ 0.8, protein expression was induced with 1mM isopropyl ®-D-thiogalactoside (IPTG) for 4 hr at 25°C. Cells were collected by centrifugation and resuspended in NETN buffer (20mM Tris-HCl, pH 8.0, 0.1M NaCl, 1mM EDTA, 0.5% NP40) plus cocktail of protease inhibitors (Roche) and lysed by sonication. The lysed cells were cleared by centrifugation and supernatants were collected. The fusion protein in the supernatant was allowed to bind to glutathione beads (Amersham) and subsequently eluted from the beads with elution buffer (20mM glutathione (Sigma), 200mM Tris-HCl, pH 8.0, 150mM NaCl). The fusion protein was concentrated by centrifugation in Centricon (Millipore) and dialyzed with PBS.

Peptide Array Analysis

Cellulose membranes modified with polyethylene glycol and Fmocprotected amino acids were purchased from Abimed (Lagenfeld, Germany). Fmoc-protected ®-alanine was purchased from Chem-Impex (Wood Dale, IL). The arrays were defined on the membranes by coupling a ®-alanine spacer and peptides were synthesized using standard DIC/HOBt coupling chemistry as described previously [58,59]. Activated amino acids were spotted using an Abimed ASP 222 robot. Washing and deprotection steps were done manually and the peptides were N-terminally acetylated after the final synthesis cycle. Following peptide synthesis and side chain deprotection, the membranes were washed in methanol for 10 min and in blocker (1 % casein in PBS) for 10 min followed by a 10-min wash in PBS. The membranes were then incubated with 110 nM GST-SLIC-1 or GST-PX for 2 hr at 4° C with gentle shaking. Control membranes were incubated with the same concentration of GST alone. The membranes were washed 4 times for 2 min in PBS at 4° C and the remaining bound protein was transferred onto a single PVDF membrane using a semi-dry blotter. The PVDF membrane was washed in blocker for 20 min and then incubated with 0.25 μg/mL of HRP-conjugated anti-GST antibody B14 (Santa Cruz) for 30 min followed by a 10-min wash with blocker and two ten minutes washes with TBS. The protein was visualized using SuperSignal West reagent (Pierce) and a digital camera (AlphaInnotech FluorImager). Signal intensity reflects the amount of protein bound at each spot.

Lipid Overlay Assay

Lipid strips and arrays were purchased from Echelon. Each membrane was first blocked in blocking buffer (10mM Tris-HCl, pH8, 150mM NaCl, 0.1% Tween-20, 3% fatty acid free BSA (Sigma) for 1 hour at room temperature. The membrane was then incubated in blocking buffer containing each GST fusion protein at 3μg/ml for 1 hour at room temperature. After three washes with the blocking buffer, the membrane was probed with an anti-GST monoclonal antibody (Santa Cruz) followed by anti-mouse IgG-HRP (Jackson's Laboratories). The bound proteins were detected using ECL reagents (NEN).

Indirect Immunofluorescent Staining and Confocal Microscopy

COS or CHO cells grown on coverslips were transfected with pEGFP plasmids expressing EGFP alone, EGFP-SLIC-1, or EGFP-SLICR116Q. In 24-48 hr post transfection, cells were fixed in 2% paraformaldehyde at 4°C for 20 min. For transferrin labeling, cells were starved for 3 hr in serum-free growth medium and incubated with 5μg/ml Texas Red-conjugated human transferrin (Molecular Probes) for 15 min before fixation. For Wortmannin labeling, cells were incubated with 100nM Wortmannin (Sigma) for indicated periods of time before fixation. For co-staining, cells were permeabilized in 0.1% Triton-X in PBS for 10 min and indirect immunofluorescent staining was carried out. Cells were incubated with primary

antibody diluted in blocking buffer (3% BSA, 10% FBS, 90% PBS) for 1 hr at 25°C. After washing three times with PBS, cells were incubated with secondary antibody diluted in blocking buffer for 1 hr at 25°C. Cells were washed three times with PBS and the coverslips were mounted on slides with Anti-Fade mounting media (Molecular Probes). For EEA1 staining, an anti-EEA1 monoclonal antibody (BD Biosciences) and Texas Red-conjugated goat anti-mouse secondary antibody (Molecular Probes) were used. For PSGL-1 staining, an anti-PSGL-1 monoclonal antibody 4H10 and Texas Red-conjugated goat anti-mouse secondary antibody (Molecular Probes) were used. Image acquisition was performed on a Nikon Eclipse TE300 microscope equipped with a Radiance 2000 confocal microscopy system and LaserSharp2000 software (BIORAD).

Generation of SLIC-1/SNX20 knockout mice

The murine homologue for human SLIC-1 was previously cloned and named SNX20. SNX20 deficient mice were designed at Wyeth Research and generated at Lexicon Genetics, Inc. from 129SvEv-Brd mice carrying a cre/loxP conditional knockout allele of the SNX20 gene. The cre recombination resulted in the deletion of exon 2 and 3, which included the transcription initiation codon ATG on exon 2. Detailed methods are included in the supplemental material.

Neutrophil Isolation

Mice in all experimental procedures were used in accordance with an approved animal care and use protocol (IACUC #11712). Mouse bone marrow was extracted from the femurs of SNX20−/− and SvEv129 wildtype mice as previously described (Lowell, JBC 1996). Briefly bone marrow was collected from experimental mice and suspended in Hank's Balanced Salt Solution (HBSS). After destroying the red blood cells using hypotonic lysis, neutrophils were purified from the resulting leukocyte population by layering the lysates on top of a 62% percoll and applying centrifugation at 1300g. The resulting neutrophils were suspended in saline buffered with 30 mM HEPES (HEPES buffer) without calcium, and the concentration of cells was determined using an automated Coulter counter (Beckton Dixon).

Flow Chamber

Vascular mimetic microfluidic flow chambers were employed in order to apply shear stress to murine neutrophils on a substrate of murine L-cells transfected with E-selectin and ICAM-1 as previously described [45,60]. Detailed methods describing how neutrophil arrest was imaged and quantified are included in the supplemental material.

Real Time Immunofluorescence

In indicated flow chamber experiments, wildtype or SNX20−/− neutrophils were incubated with 10 μg/mL rat anti mouse-PSGL-1 (2PH-1, BD Biosciences) conjugated to PE for 10 minutes at room temperature before infusion. The antibody did not block interaction between neutrophils and the L-E monolayer, allowing real-time imaging of PSGL-1 localization by mercury lamp equipped fluorescent videomicroscopy with appropriate filters. PSGL-1 clusters on the neutrophils captured in the resulting image sequences were defined as continuous regions 2.5 standard deviations brighter than the whole-cell average. Sequences were analyzed for cluster size, number of clusters, and average cluster distance from the centroid using a custom macro written for Image Pro Plus.

Detection of PSGL-1 Dependent Calcium Flux

In order to detect early neutrophil activation due to crosslinking of PSGL-1, we employed flow cytometry to measure calcium flux. The average level of intracellular calcium in stimulated neutrophils was assayed using the calcium sensitive dye Fluo-4. Neutrophils were

incubated with 1 μM Fluo-4 AM in calcium free HEPES buffer for 30 minutes at 37°C. After this loading step, the cells were pelleted and then resuspended in HEPES buffer containing 1.5 mM calcium to a concentration of 2×10^6 neutrophils/mL. At this point, neutrophils were incubated with 40 μg/mL of either a primary anti-PSGL-1 antibody (2PH-1) or an isotype matched rat IgG (Southern Biotech) on ice for 20 minutes. Neutrophils were then pelleted and resuspended in HEPES buffer containing 25 mg/mL of secondary goat anti-rat IgG (Southern Biotech) and 1.5 mM calcium, then incubated for 20 minutes on ice. PSGL-1 crosslinked and control samples were then warmed to 37°C for 1 minute before sampling by flow cytometry. Certain samples were exposed to 5 nM MIP-1α at this point as a positive activation control. The FITC channel was recorded for all neutrophils after excitation on a FACScan single laser cytometer over the course of 10 minutes at 37°C. Calcium flux was quantified as the fraction of neutrophils exhibiting Fluo-4 intensity 2 times greater than the average unstimulated neutrophils.

Supplementary Material

Refer to Web version on PubMed Central for supplementary material.

Acknowledgments

We thank Richard Konz, Tony Li, and James Graham, and Kristie Bridges for technical help and Robert Schaub for support and advice. We gratefully acknowledge NIH support to SIS AI47294. Funding for this research was also provided by Wyeth.

Abbreviations

SLIC-1	selectin ligand interactor cytoplasmic-1
PSGL-1	P-selectin glycoprotein ligand-1
SNX	sorting nexin
PX domain	phox homology domain
PCR	polymerase chain reaction
FBS	fetal bovine serum
GST	glutathione S-transferase
EGFP	enhanced green fluorescence protein
EEA-1	early endosomal antigen-1
ERM	ezrin/radixin/moesin
TM	transmembrane
PI	phosphatidylinositol
PtdIns(3)P	phosphatidylinositol 3-phosphate
PtdIns(4)P	phosphatidylinositol 4-phosphate
PtdIns(5)P	phosphatidylinositol 5-phosphate
PtdIns(3, 4)P_2	phosphatidylinositol 3,4-biphosphate
PtdIns(3,5)P_2	phosphatidylinositol 3,5-biphosphate
PtdIns(4, 5)P_2	phosphatidylinositol 4,5-biphosphate
PtdIns(3, 4, 5)P_3	phosphatidylinositol 3,4,5-triphosphate

PI-3 kinase	phosphatidylinositol-3 kinase

REFERENCES

1. McEver RP. Selectin-carbohydrate interactions during inflammation and metastasis. Glycoconj J. 1997; 14:585–591. [PubMed: 9298691]
2. McEver RP. P-selectin and PSGL-1: exploiting connections between inflammation and venous thrombosis. Thromb Haemost. 2002; 87:364–365. [PubMed: 11916065]
3. McEver RP, Cummings RD. Perspectives series: cell adhesion in vascular biology. Role of PSGL-1 binding to selectins in leukocyte recruitment. J Clin Invest. 1997; 100:485–491. [PubMed: 9239393]
4. Yang J, Furie BC, Furie B. The biology of P-selectin glycoprotein ligand-1: its role as a selectin counterreceptor in leukocyte-endothelial and leukocyte-platelet interaction. Thromb Haemost. 1999; 81:1–7. [PubMed: 10348699]
5. Sako D, Comess KM, Barone KM, Camphausen RT, Cumming DA, Shaw GD. A sulfated peptide segment at the amino terminus of PSGL-1 is critical for P-selectin binding. Cell. 1995; 83:323–331. [PubMed: 7585949]
6. Li F, Erickson HP, James JA, Moore KL, Cummings RD, McEver RP. Visualization of P-selectin glycoprotein ligand-1 as a highly extended molecule and mapping of protein epitopes for monoclonal antibodies. J Biol Chem. 1996; 271:6342–6348. [PubMed: 8626430]
7. Liu W, Ramachandran V, Kang J, Kishimoto TK, Cummings RD, McEver RP. Identification of N-terminal residues on P-selectin glycoprotein ligand-1 required for binding to P-selectin. J Biol Chem. 1998; 273:7078–7087. [PubMed: 9507018]
8. Patel KD, Nollert MU, McEver RP. P-selectin must extend a sufficient length from the plasma membrane to mediate rolling of neutrophils. J Cell Biol. 1995; 131:1893–1902. [PubMed: 8557755]
9. Wilkins PP, McEver RP, Cummings RD. Structures of the O-glycans on P-selectin glycoprotein ligand-1 from HL-60 cells. J Biol Chem. 1996; 271:18732–18742. [PubMed: 8702529]
10. Wilkins PP, Moore KL, McEver RP, Cummings RD. Tyrosine sulfation of P-selectin glycoprotein ligand-1 is required for high affinity binding to P-selectin. J Biol Chem. 1995; 270:22677–22680. [PubMed: 7559387]
11. Haller H, Kunzendorf U, Sacherer K, Lindschau C, Walz G, Distler A, Luft FC. T cell adhesion to P-selectin induces tyrosine phosphorylation of pp125 focal adhesion kinase and other substrates. J Immunol. 1997; 158:1061–1067. [PubMed: 9013943]
12. Evangelista V, Manarini S, Sideri R, Rotondo S, Martelli N, Piccoli A, Totani L, Piccardoni P, Vestweber D, de Gaetano G, Cerletti C. Platelet/polymorphonuclear leukocyte interaction: P-selectin triggers protein-tyrosine phosphorylation-dependent CD11b/CD18 adhesion: role of PSGL-1 as a signaling molecule. Blood. 1999; 93:876–885. [PubMed: 9920836]
13. Hidari KI, Weyrich AS, Zimmerman GA, McEver RP. Engagement of P-selectin glycoprotein ligand-1 enhances tyrosine phosphorylation and activates mitogen-activated protein kinases in human neutrophils. J Biol Chem. 1997; 272:28750–28756. [PubMed: 9353345]
14. Snapp KR, Heitzig CE, Kansas GS. Attachment of the PSGL-1 cytoplasmic domain to the actin cytoskeleton is essential for leukocyte rolling on P-selectin. Blood. 2002; 99:4494–4502. [PubMed: 12036880]
15. Moore KL, Patel KD, Bruehl RE, Li F, Johnson DA, Lichenstein HS, Cummings RD, Bainton DF, McEver RP. P-selectin glycoprotein ligand-1 mediates rolling of human neutrophils on P-selectin. J Cell Biol. 1995; 128:661–671. [PubMed: 7532174]
16. Bruehl RE, Moore KL, Lorant DE, Borregaard N, Zimmerman GA, McEver RP, Bainton DF. Leukocyte activation induces surface redistribution of P-selectin glycoprotein ligand-1. J Leukoc Biol. 1997; 61:489–499. [PubMed: 9103236]
17. Lorant DE, McEver RP, McIntyre TM, Moore KL, Prescott SM, Zimmerman GA. Activation of polymorphonuclear leukocytes reduces their adhesion to P-selectin and causes redistribution of ligands for P-selectin on their surfaces. J Clin Invest. 1995; 96:171–182. [PubMed: 7542276]

18. Teasdale RD, Loci D, Houghton F, Karlsson L, Gleeson PA. A large family of endosome-localized proteins related to sorting nexin 1. Biochem J. 2001; 358:7–16. [PubMed: 11485546]
19. Worby CA, Dixon JE. Sorting out the cellular functions of sorting nexins. Nat Rev Mol Cell Biol. 2002; 3:919–931. [PubMed: 12461558]
20. Xu Y, Seet LF, Hanson B, Hong W. The Phox homology (PX) domain, a new player in phosphoinositide signalling. Biochem J. 2001; 360:513–530. [PubMed: 11736640]
21. Kanai F, Liu H, Field SJ, Akbary H, Matsuo T, Brown GE, Cantley LC, Yaffe MB. The PX domains of p47phox and p40phox bind to lipid products of PI(3)K. Nat Cell Biol. 2001; 3:675–678. [PubMed: 11433300]
22. Ponting CP. Novel domains in NADPH oxidase subunits, sorting nexins, and PtdIns 3-kinases: binding partners of SH3 domains? Protein Sci. 1996; 5:2353–2357. [PubMed: 8931154]
23. Stockinger W, Sailler B, Strasser V, Recheis B, Fasching D, Kahr L, Schneider WJ, Nimpf J. The PX-domain protein SNX17 interacts with members of the LDL receptor family and modulates endocytosis of the LDL receptor. Embo J. 2002; 21:4259–4267. [PubMed: 12169628]
24. Zheng B, Ma YC, Ostrom RS, Lavoie C, Gill GN, Insel PA, Huang XY, Farquhar MG. RGS-PX1, a GAP for GalphaS and sorting nexin in vesicular trafficking. Science. 2001; 294:1939–1942. [PubMed: 11729322]
25. Florian V, Schluter T, Bohnensack R. A new member of the sorting nexin family interacts with the C-terminus of P-selectin. Biochem Biophys Res Commun. 2001; 281:1045–1050. [PubMed: 11237770]
26. Kurten RC, Cadena DL, Gill GN. Enhanced degradation of EGF receptors by a sorting nexin, SNX1. Science. 1996; 272:1008–1010. [PubMed: 8638121]
27. Otsuki T, Kajigaya S, Ozawa K, Liu JM. SNX5, a new member of the sorting nexin family, binds to the Fanconi anemia complementation group A protein. Biochem Biophys Res Commun. 1999; 265:630–635. [PubMed: 10600472]
28. Parks WT, Frank DB, Huff C, Renfrew Haft C, Martin J, Meng X, de Caestecker MP, McNally JG, Reddi A, Taylor SI, Roberts AB, Wang T, Lechleider RJ. Sorting nexin 6, a novel SNX, interacts with the transforming growth factor-beta family of receptor serine-threonine kinases. J Biol Chem. 2001; 276:19332–19339. [PubMed: 11279102]
29. Phillips SA, Barr VA, Haft DH, Taylor SI, Haft CR. Identification and characterization of SNX15, a novel sorting nexin involved in protein trafficking. J Biol Chem. 2001; 276:5074–5084. [PubMed: 11085978]
30. Xu J, Liu D, Gill G, Songyang Z. Regulation of cytokine-independent survival kinase (CISK) by the Phox homology domain and phosphoinositides. J Cell Biol. 2001; 154:699–705. [PubMed: 11514587]
31. Ellson CD, Gobert-Gosse S, Anderson KE, Davidson K, Erdjument-Bromage H, Tempst P, Thuring JW, Cooper MA, Lim ZY, Holmes AB, Gaffney PR, Coadwell J, Chilvers ER, Hawkins PT, Stephens LR. PtdIns(3)P regulates the neutrophil oxidase complex by binding to the PX domain of p40(phox). Nat Cell Biol. 2001; 3:679–682. [PubMed: 11433301]
32. Haft CR, de la Luz Sierra M, Barr VA, Haft DH, Taylor SI. Identification of a family of sorting nexin molecules and characterization of their association with receptors. Mol Cell Biol. 1998; 18:7278–7287. [PubMed: 9819414]
33. Xu Y, Hortsman H, Seet L, Wong SH, Hong W. SNX3 regulates endosomal function through its PX-domain-mediated interaction with PtdIns(3)P. Nat Cell Biol. 2001; 3:658–666. [PubMed: 11433298]
34. Ellson CD, Andrews S, Stephens LR, Hawkins PT. The PX domain: a new phosphoinositide-binding module. J Cell Sci. 2002; 115:1099–1105. [PubMed: 11884510]
35. Sato TK, Overduin M, Emr SD. Location, location, location: membrane targeting directed by PX domains. Science. 2001; 294:1881–1885. [PubMed: 11729306]
36. Wishart MJ, Taylor GS, Dixon JE. Phoxy lipids: revealing PX domains as phosphoinositide binding modules. Cell. 2001; 105:817–820. [PubMed: 11439176]
37. Zeng W, Yuan W, Wang Y, Jiao W, Zhu Y, Huang C, Li D, Li Y, Zhu C, Wu X, Liu M. Expression of a novel member of sorting nexin gene family, SNX-L, in human liver development. Biochem Biophys Res Commun. 2002; 299:542–548. [PubMed: 12459172]

38. Bruehl RE, Springer TA, Bainton DF. Quantitation of L-selectin distribution on human leukocyte microvilli by immunogold labeling and electron microscopy. J Histochem Cytochem. 1996; 44:835–844. [PubMed: 8756756]
39. Erlandsen SL, Hasslen SR, Nelson RD. Detection and spatial distribution of the beta 2 integrin (Mac-1) and L-selectin (LECAM-1) adherence receptors on human neutrophils by high-resolution field emission SEM. J Histochem Cytochem. 1993; 41:327–333. [PubMed: 7679125]
40. Picker LJ, Warnock RA, Burns AR, Doerschuk CM, Berg EL, Butcher EC. The neutrophil selectin LECAM-1 presents carbohydrate ligands to the vascular selectins ELAM-1 and GMP-140. Cell. 1991; 66:921–933. [PubMed: 1716182]
41. Alonso-Lebrero JL, Serrador JM, Dominguez-Jimenez C, Barreiro O, Luque A, del Pozo MA, Snapp K, Kansas G, Schwartz-Albiez R, Furthmayr H, Lozano F, Sanchez-Madrid F. Polarization and interaction of adhesion molecules P-selectin glycoprotein ligand 1 and intercellular adhesion molecule 3 with moesin and ezrin in myeloid cells. Blood. 2000; 95:2413–2419. [PubMed: 10733515]
42. Serrador JM, Urzainqui A, Alonso-Lebrero JL, Cabrero JR, Montoya MC, Vicente-Manzanares M, Yanez-Mo M, Sanchez-Madrid F. A juxta-membrane amino acid sequence of P-selectin glycoprotein ligand-1 is involved in moesin binding and ezrin/radixin/moesin-directed targeting at the trailing edge of migrating lymphocytes. Eur J Immunol. 2002; 32:1560–1566. [PubMed: 12115638]
43. Bravo J, Karathanassis D, Pacold CM, Pacold ME, Ellson CD, Anderson KE, Butler PJ, Lavenir I, Perisic O, Hawkins PT, Stephens L, Williams RL. The crystal structure of the PX domain from p40(phox) bound to phosphatidylinositol 3-phosphate. Mol Cell. 2001; 8:829–839. [PubMed: 11684018]
44. Kumar R, Camphausen RT, Sullivan FX, Cumming DA. Core2 beta-1,6-N-acetylglucosaminyltransferase enzyme activity is critical for P-selectin glycoprotein ligand-1 binding to P-selectin. Blood. 1996; 88:3872–3879. [PubMed: 8916952]
45. Simon SI, Hu Y, Vestweber D, Smith CW. Neutrophil tethering on E-selectin activates beta 2 integrin binding to ICAM-1 through a mitogen-activated protein kinase signal transduction pathway. J Immunol. 2000; 164:4348–4358. [PubMed: 10754335]
46. Green CE, Pearson DN, Camphausen RT, Staunton DE, Simon SI. Shear-dependent capping of L-selectin and P-selectin glycoprotein ligand 1 by E-selectin signals activation of high-avidity beta2-integrin on neutrophils. J Immunol. 2004; 172:7780–7790. [PubMed: 15187162]
47. Sikorski EE, Hallmann R, Berg EL, Butcher EC. The Peyer's patch high endothelial receptor for lymphocytes, the mucosal vascular addressin, is induced on a murine endothelial cell line by tumor necrosis factor-alpha and IL-1. J Immunol. 1993; 151:5239–5250. [PubMed: 7693807]
48. Blanks JE, Moll T, Eytner R, Vestweber D. Stimulation of P-selectin glycoprotein ligand-1 on mouse neutrophils activates beta 2-integrin mediated cell attachment to ICAM-1. Eur J Immunol. 1998; 28:433–443. [PubMed: 9521050]
49. Wang XG, Cheng YP, Ba XQ. Engagement of PSGL-1 enhances beta(2)-integrin-involved adhesion of neutrophils to recombinant ICAM-1. Acta Pharmacol Sin. 2006; 27:617–622. [PubMed: 16626518]
50. Seet LF, Hong W. The Phox (PX) domain proteins and membrane traffic. Biochim Biophys Acta. 2006; 1761:878–896. [PubMed: 16782399]
51. Verges M. Retromer and sorting nexins in development. Front Biosci. 2007; 12:3825–3851. [PubMed: 17485342]
52. Roche PA. Intracellular protein traffic in lymphocytes: “how do I get THERE from HERE”? Immunity. 1999; 11:391–398. [PubMed: 10549621]
53. van Kerkhof P, Lee J, McCormick L, Tetrault E, Lu W, Schoenfish M, Oorschot V, Strous GJ, Klumperman J, Bu G. Sorting nexin 17 facilitates LRP recycling in the early endosome. Embo J. 2005; 24:2851–2861. [PubMed: 16052210]
54. Urzainqui A, Serrador JM, Viedma F, Yanez-Mo M, Rodriguez A, Corbi AL, Alonso-Lebrero JL, Luque A, Deckert M, Vazquez J, Sanchez-Madrid F. ITAM-based interaction of ERM proteins with Syk mediates signaling by the leukocyte adhesion receptor PSGL-1. Immunity. 2002; 17:401–412. [PubMed: 12387735]

55. Schwarz DG, Griffin CT, Schneider EA, Yee D, Magnuson T. Genetic analysis of sorting nexins 1 and 2 reveals a redundant and essential function in mice. Mol Biol Cell. 2002; 13:3588–3600. [PubMed: 12388759]

56. Zheng B, Tang T, Tang N, Kudlicka K, Ohtsubo K, Ma P, Marth JD, Farquhar MG, Lehtonen E. Essential role of RGS-PX1/sorting nexin 13 in mouse development and regulation of endocytosis dynamics. Proc Natl Acad Sci U S A. 2006; 103:16776–16781. [PubMed: 17077144]

57. Khor SP, McCarthy K, DuPont M, Murray K, Timony G. Pharmacokinetics, pharmacodynamics, allometry, and dose selection of rPSGL-Ig for phase I trial. J Pharmacol Exp Ther. 2000; 293:618–624. [PubMed: 10773036]

58. Frank R. An easy technique for the positionally addressable parallel chemical synthesis on a membrane support. Tetrahedron. 1992; 48:9217–9232.

59. Molina F, Laune D, Gougat C, Pau B, Granier C. Improved performances of spot multiple peptide synthesis. Pept Res. 1996; 9:151–155. [PubMed: 8875595]

60. Schaff UY, Xing MM, Lin KK, Pan N, Jeon NL, Simon SI. Vascular mimetics based on microfluidics for imaging the leukocyte--endothelial inflammatory response. Lab Chip. 2007; 7:448–456. [PubMed: 17389960]

61. Serrador JM, Vicente-Manzanares M, Calvo J, Barreiro O, Montoya MC, Schwartz-Albiez R, Furthmayr H, Lozano F, Sanchez-Madrid F. A novel serine-rich motif in the intercellular adhesion molecule 3 is critical for its ezrin/radixin/moesin-directed subcellular targeting. J Biol Chem. 2002; 277:10400–10409. [PubMed: 11784723]

62. Moore KL, Eaton SF, Lyons DE, Lichenstein HS, Cummings RD, McEver RP. The P-selectin glycoprotein ligand from human neutrophils displays sialylated, fucosylated, O-linked poly-N-acetyllactosamine. J Biol Chem. 1994; 269:23318–23327. [PubMed: 7521878]

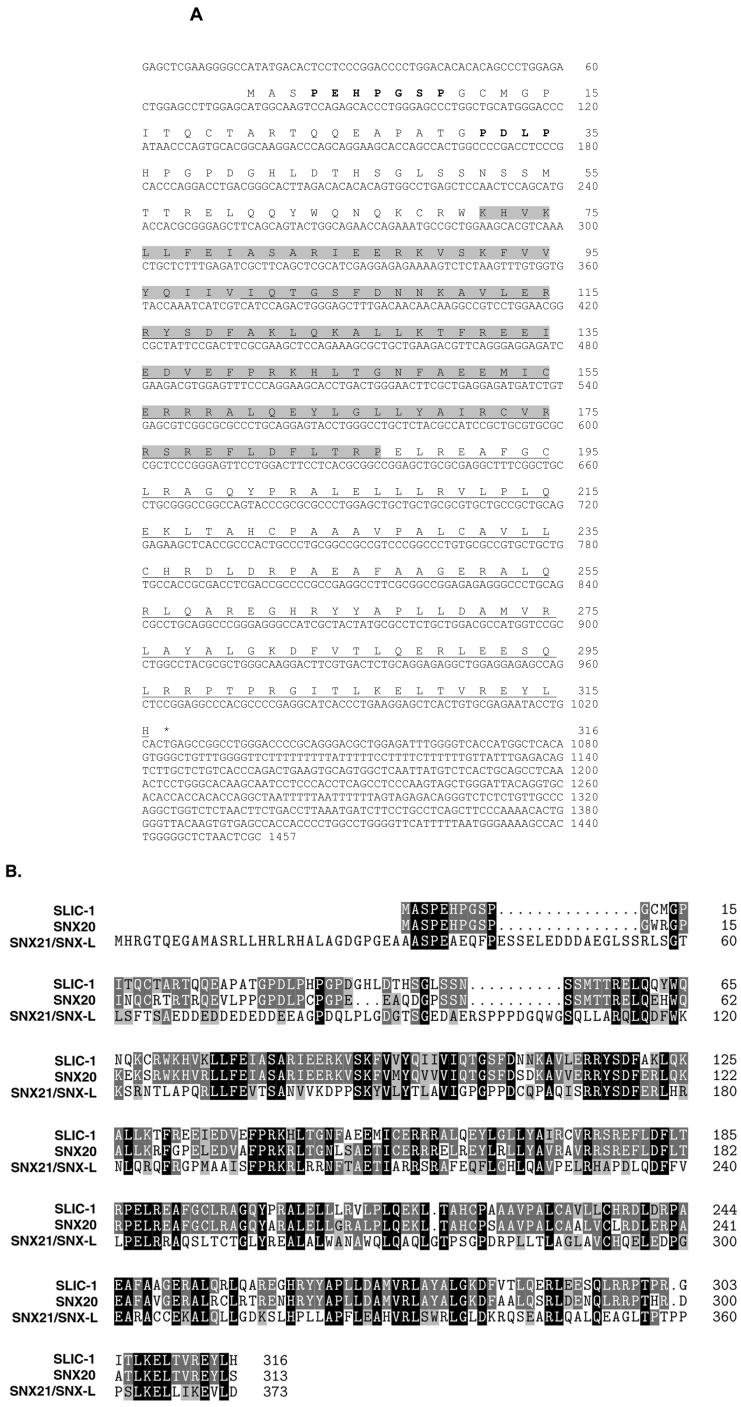

Fig. 1. Sequence of human SLIC-1

(A) Nucleotide and predicted amino acid sequences of human SLIC-1. The PX domain is shaded. PXXP motifs are in bold. The amino acid sequences obtained from the yeast two-hybrid screen are underlined. (B) The amino acid sequences of human SLIC-1 and its mouse homologue SNX20 as well as a homologous human protein SNX21/SNX-L were aligned using the CLUSTALW program. Residues completely conserved in all three proteins are

shaded in black. Those completely conserved in two proteins are shaded in dark gray. Moderately conserved residues are shaded in light gray.

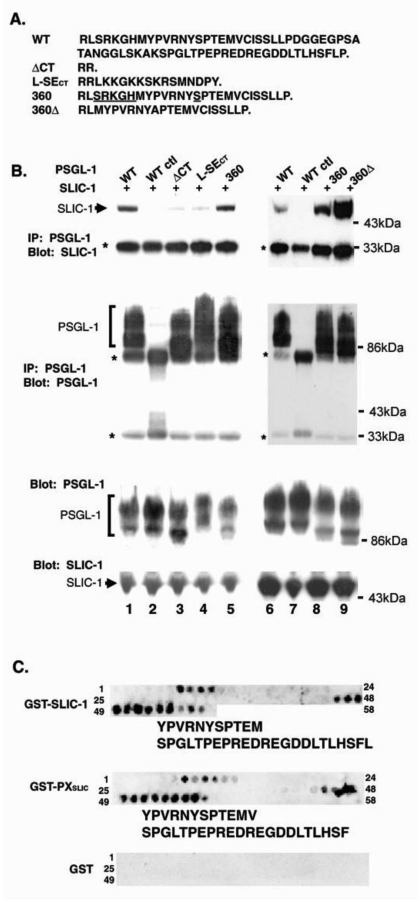

Fig. 2. SLIC-1 interacts with PSGL-1 in mammalian cells

(A) Amino acid sequences of the cytoplasmic domains of wildtype and mutant PSGL-1 proteins used in the coimmunoprecipitation experiments. The previously identified ERM interaction motif is underlined.[61] (B) SLIC-1 and wildtype or mutant PSGL-1 were coexpressed in COS cells. Cell extracts were subjected to immunoprecipitation with a mouse monoclonal anti-PSGL-1 antibody. The presence of SLIC-1 and PSGL-1 in the immunocomplex was analyzed by Western blot analysis following reducing SDS-PAGE (Top 4 panels). The total levels of over-expressed SLIC-1 and PSGL-1 in the cell extracts were analyzed by Western blot analysis (bottom four panels). SLIC-1 runs higher on SDS-PAGE gel (slightly above 43kDA molecular weight marker) than its predicted molecular weight (36kDa). The reason for this molecular weight shift remains unclear. PSGL-1 appears as a ladder of bands due to its extensive post-translational modification.[62] * denotes background IgG bands. (C) A total of 45 12-amino acid peptides representing overlapping sequences in the cytoplasmic domain of PSGL-1 were synthesized onto cellulose membranes, which were probed with indicated GST fusion proteins expressed and purified from *E. Coli*. Peptides that showed positive interactions are numbered on the right. Deduced amino acid sequences for each interaction motif are shown beneath each panel. (Sections relating to 2C.a and 2D deleted).

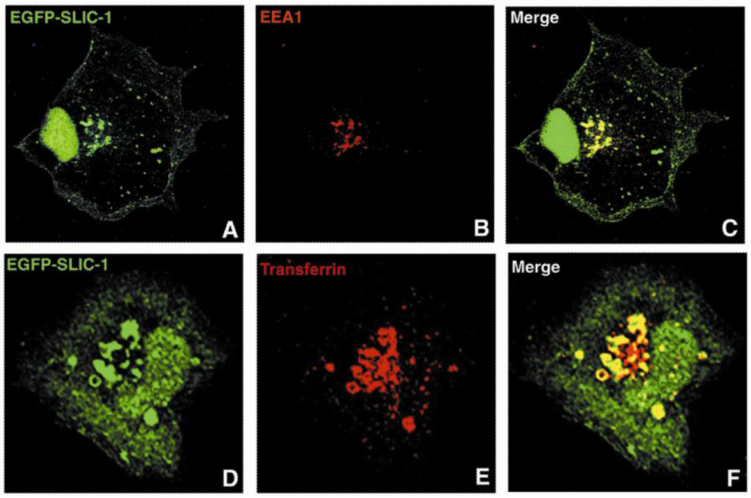

Fig. 3. SLIC-1 localizes to endosomes

COS cells were transfected with EGFP-SLIC1. For EEA1 co-staining, cells were fixed with 2% paraformaldehyde and permeabilized with 0.1% Triton-X. Indirect immunofluorescent staining was carried out using a mouse anti-EEA1 monoclonal antibody and Texas Red-conjugated goat anti-mouse antibody. A representative COS cell expressing EGFP-SLIC-1 is shown in green (A). EEA1 staining of the same cell is shown in red (B). Yellow in C indicates co-localization of SLIC-1 and EEA1 when images A and B are merged. For transferrin labeling, cells were starved for 3 hr before they were labeled with Texas Red-conjugated transferrin for 15 min. Cells were fixed and confocal microscopy was performed to analyze co-localization. One representative COS cells expressing EGFPSLIC-1 is shown in green (D). Transferrin labeling of the same cell is shown in red (E). Yellow in F indicates co-localization of SLIC-1 and transferrin when images D and E are merged.

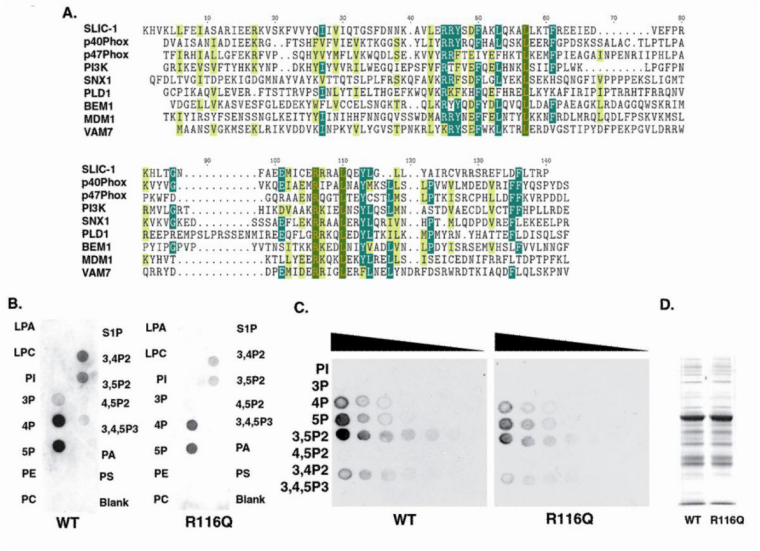

Fig. 4. The PX domain of SLIC-1 is a phospholipid-binding module

(A) Sequences of PX domains from different proteins were aligned using CLUSTAIW program. Most, moderately, and less conserved residues are shown in yellow letters on green background, white letters on green background, and black letters on yellow background, respectively. (B-D) Wildtype and R116Q mutant SLIC-1 PX domain fused C-terminally to GST were expressed and purified from *E. Coli*. The levels of these proteins were examined on a coomossie-stained SDS-PAGE gel (D). Their lipid binding activities were tested in a lipid overlay assays using commercial lipid strips (B) or lipid arrays (C). Concentration of each lipid spot on the lipid strip was 100pmol. Concentrations of lipids used for spotting each lipid array were 100pmol, 50pmol, 25pmol, 12.5pmol, 6.3pmol, 3.2pmol, and 1.6pmol. LPA, lysophosphatidic acid; LPC, lysophosphocholine; S1P, sphingosine-1-phosphate; PE, phosphatidylethanolamine; PA, phosphatidic acid; PC, phosphatidylcholine; PS, phosphatidylserine, PI, phosphoinositide.

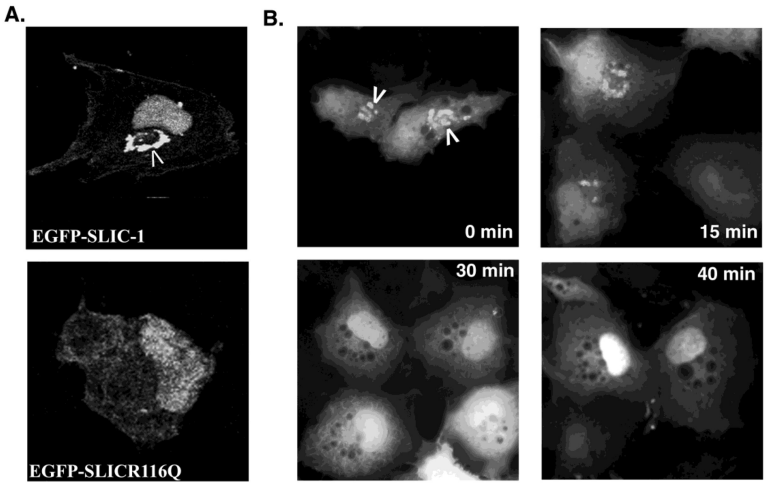

Fig. 5. Endosomal localization of SLIC-1 is dependent on phospholipid binding

(A) COS cells were transfected with pEGFP-C1-SLIC-1 or pEGFP-C1-SLICR116Q. In 24 hr post transfection, cells were fixed and subjected to confocal microscopy. Top panel: One representative COS cells expressing EGFP-SLIC-1; Bottom panel: Three representative COS cells expressing EGFP-SLICR116Q. (B) COS cells transfected with EGFP-SLIC-1 were treated with Wortmannin for indicated periods of time and analyzed by fluorescent microscopy. Bright staining shows EGFP-SLIC-1 positive cells.

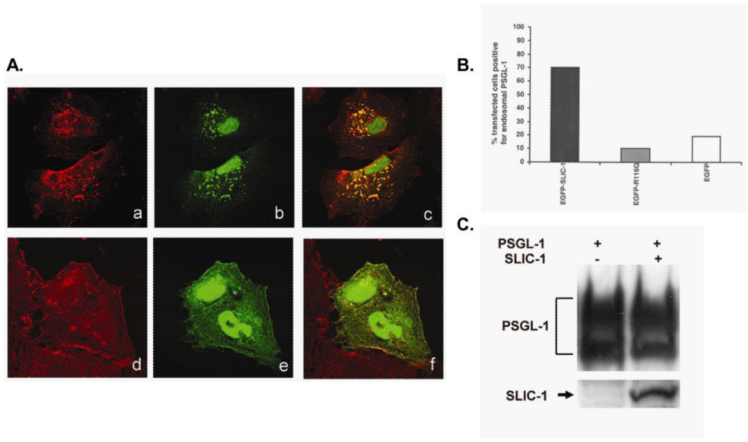

Fig. 6. SLIC-1 affects PSGL-1 subcellular localization

(A) CHO cells stably expressing PSGL-1 were transfected with pEGFP-C1-SLIC-1 (a, b, c) or pEGFP-C1-SLICR116Q (d, e, f). In 24 hr after transfection, cells were fixed, permeabilized, and subjected to indirect immunofluorescent staining with a mouse anti-PSGL-1 monoclonal antibody and Texas Red-conjugated goat anti-mouse antibody. Confocal microscopy was performed to visualize PSGL-1 staining in red (a, d), and EGFP-SLIC-1 (b) or EGFP-SLICR116Q (e) in green. Panels c and f represented merged images. Experiment was repeated four times and similar results were obtained. (B) One hundred cells from one representative experiment in A were counted under fluorescence microscope. Percentage of cells that showed PSGL-1 staining in vesicles among transfected cells (green cells) was calculated and shown in the bar graph. (C) COS cells were transfected with plasmid expressing PSGL-1 in the presence or absence of SLIC-1. Cell lysates were separated by SDS-PAGE and Western analysis was carried out to determine the total levels of PSGL-1.

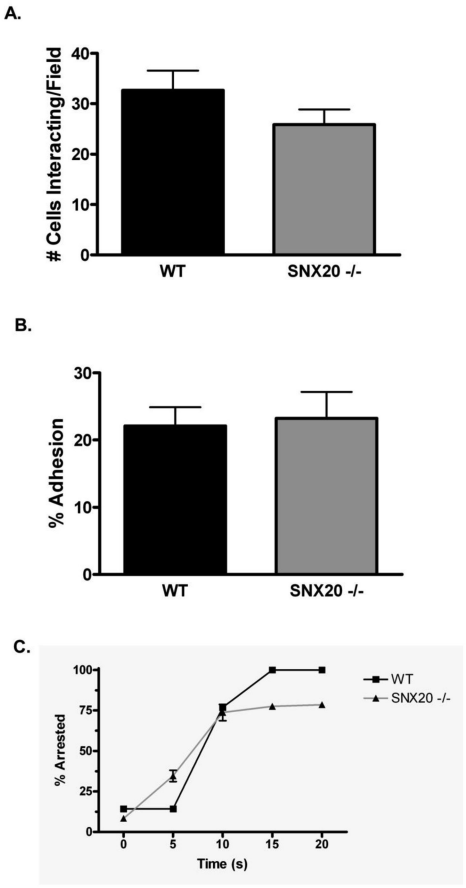

Fig 7. SNX20 −/− neutrophils exhibit normal recruitment to cell monolayers expressing E-selectin and ICAM-1

Murine bone marrow neutrophils were perfused over a cell monolayer expressing E-selectin and ICAM-1, and their subsequent rolling and arrest was recorded by phase contrast videomicroscopy. (A, B) There was no significant difference ($p>0.05$) between the number of wildtype or SNX20 deficient neutrophils that rolled or transitioned to arrest in an average microscope field under 1 dyne/cm^2 shear stress. (C) When exposed to 0.1 nM MIP1a, SNX20 −/− and wildtype neutrophils were equally capable of transitioning from rolling to firm arrest with high efficiency. Data was representative of 6 experimental runs, each of which was the average of 6 microscope fields over the course of 6 minutes.

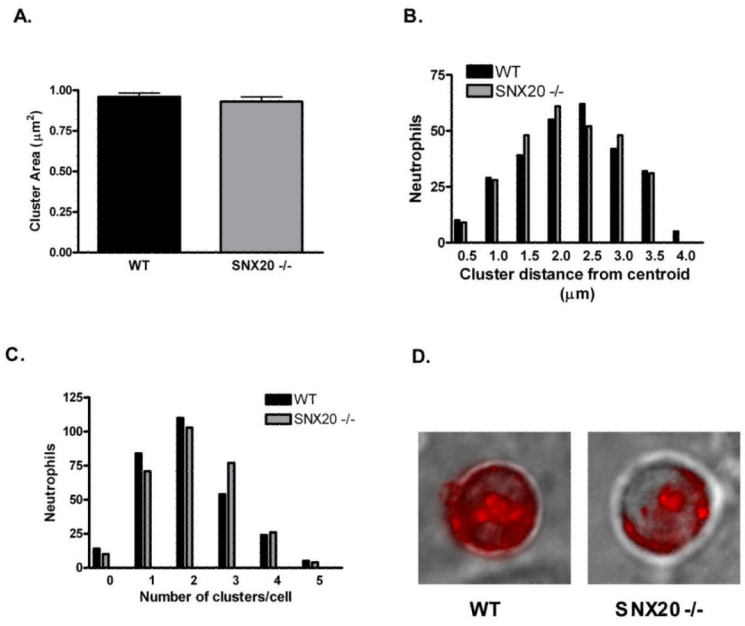

Fig 8. Absence of SNX20 does not affect surface distribution of PSGL-1 in murine neutrophils interacting with E-selectin and ICAM-1

Murine neutrophils were labeled were perfused over an L-E/I monolayer, allowed to roll and arrest, and then labeled with anti-PSGL-1 conjugated to PE. Distribution of PSGL-1 was imaged by immunofluorescent microscopy. (A, B) Clusters of PSGL-1 (defined as regions 2.5 standard deviations higher than background) covered the same total surface area and had the same distribution of distances from the cell centroid between SNX20 −/− and wildtype neutrophils rolling on an L-E/I monolayer. (C) There was no significant difference in the average number of clusters between the two cell types. (D) Sample images show a representative image of PSGL-1 distribution on the surface of a rolling neutrophil. Data was based on a total of 290 neutrophils for each condition. There was no significant difference between the average values for wildtype and SNX20 −/− neutrophils in cluster size, number of clusters, or cluster distance from centroid.

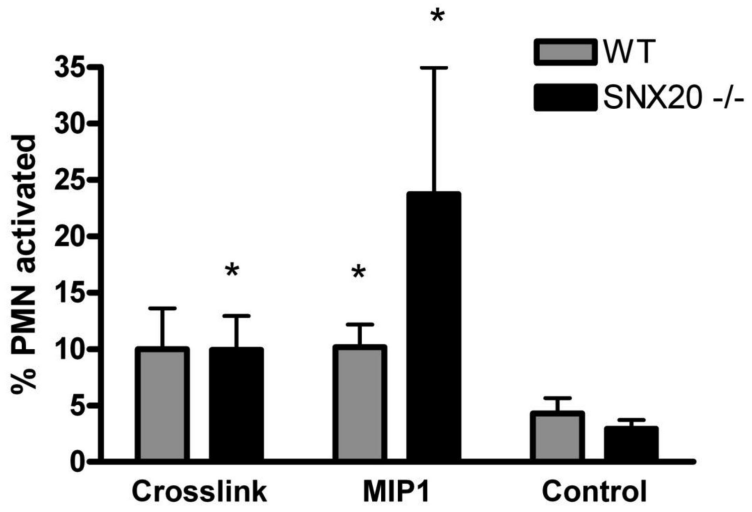

Fig 9. PSGL-1 crosslinking induces calcium flux in neutrophils which is unaffected by SNX20 deficiency

Murine neutrophils were loaded with calcium sensitive Fluo-4 dye, treated with anti-PSGL-1 and a secondary crosslinker, then analyzed for calcium flux by flow cytometry. The fraction of Fluo-4 stained neutrophils above an intensity threshold was plotted for SNX20 −/− and wildtype neutrophils after PSGL-1 or control antibody crosslinking treatment over a period of 10 minutes. After 160 seconds, both SNX20 −/− and wildtype neutrophils exhibited greater calcium flux than the unstimulated controls. There was no significant difference in the calcium flux between SNX20 −/− or wildtype neutrophils, while the conditions marked with * exhibited significantly more calcium flux ($p<0.05$) than the respective neutrophil type (WT or SNX −/−) in the absence of antibody crosslinking (control IgG).